VIP Alkaline-Stable Benzimidazolium | Very Important Paper

International Edition: DOI: 10.1002/anie.201511184
German Edition: DOI: 10.1002/ange.201511184

# Poly(phenylene) and *m*-Terphenyl as Powerful Protecting Groups for the Preparation of Stable Organic Hydroxides

*Andrew G. Wright, Thomas Weissbach, and Steven Holdcroft**

***Abstract:*** *Four benzimidazolium hydroxide compounds, in which the C2-position is attached to a phenyl group possessing hydrogen, bromine, methyl groups, or phenyl groups at the ortho positions, are prepared and investigated for stability in a quantitative alkaline stability test. The differences between the stability of the various protecting groups in caustic solutions are rationalized on the basis of their crystal structures and DFT calculations. The highest stability was observed for the m-terphenyl-protected benzimidazolium, showing a half-life in 3 M $NaOD/CD_3OD/D_2O$ at 80 °C of 3240 h. A high-molecular-weight polymer analogue of this model compound is prepared that exhibits excellent mechanical properties, high ionic conductivity and ion-exchange capacity, as well as remarkable hydroxide stability in alkaline solutions: only 5 % degradation after 168 h in 2 M KOH at 80 °C. This is the most stable hydroxide-conducting benzimidazolium polymer to date.*

Immobilized quaternary ammoniums are a class of cationic head groups that support the conduction of anions.[1–7] They have been used in a range of technologies, such as anion-exchange resins,[8] hydrogen fuel cells,[1,9,10] water electrolyzers,[11] redox-flow batteries,[12] and reverse dialysis.[13] However, of the numerous reported cationic groups,[14,15] only a few show promise of long term stability under strong alkaline conditions at elevated temperatures (for example, 80 °C). A sub-class of cationic head groups that are attracting increasing attention is sterically protected imidazoliums and benzimidazoliums.

The first example of a benzimidazolium that showed promise of stability in strongly alkaline conditions was reported in 2012. The compound, **MeB** (Figure 1), bears two methyl groups, each attached to the *ortho*-position of an adjoining C2-substituted phenyl. Both the small molecule and the analogously structured polymer were found to be stable for extended periods in 2 M $KOH_{aq}$ at 60 °C.[16] The methyl groups serve to increase the dihedral angle compared to that of **HB** and sterically-protect the C2 position from hydroxide attack and its subsequent ring-opening degradation. The stability of these molecules was supported by density functional theory (DFT) calculations of Long and Pivovar, showing that methyl protecting groups greatly enhance the stability of imidazolium and benzimidazolium hydroxides

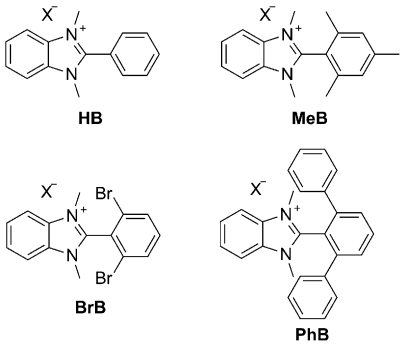


***Figure 1.*** Chemical structures of four C2-substituted benzimidazoliums prepared herein, where $X^-$ is the counteranion.

over that of quaternary ammoniums.[17] In 2015, Coates et al. demonstrated that the same *o*-dimethylphenyl C2 protecting groups also protect imidazolium molecules.[18] To date, only three polymers have been reported that utilize this type of C2-protection strategy for (benz)imidazoliums,[3,16,19] yet it provides the most likely strategy towards alkaline-stable, hydroxide-conducting polymers. The discovery that *o*-dimethylphenylenes can protect the C2 position opens the door to other *o*-substituted phenylene variants, such as halogen or aryl protecting groups.[20,21]

Herein, we present differences in hydroxide stability of four *o*-substituted phenylene C2 groups, each bearing either *ortho*-positioned hydrogen atoms (**HB**), bromine atoms (**BrB**), methyl groups (**MeB**), or phenyl groups (**PhB**). As **BrB** and **PhB** had never been reported, a novel and versatile synthetic route (Scheme 1) was designed to prepare functionalized aryl-protected benzimidazoliums on a multi-gram scale. After directed *ortho*-metalation and electrophilic aromatic substitution of 1,3-dibromobenzene,[22] an acid condensation yields compound **2** in near quantitative yield. The controlled methylation of **2** to produce **3** allows access, via Suzuki coupling, to various aryl-protected benzimidazoles, such as **4** and **5**. A second methylation of **3** and **4** yields **BrB** and **PhB**, respectively. **MeB** and **HB** were prepared according to the Supporting Information, Schemes S1 and S2.

Each of the four model compounds (Figure 1) was subjected to the same accelerated hydroxide stability test, which involved dissolution of the model compound (0.02 M) in 3 M $NaOD/CD_3OD/D_2O$ (7:3 $CD_3OD$:$D_2O$ by mass). The solutions were heated to 80 °C for up to 240 h. Aliquots were intermittently extracted and analyzed by $^1H$ NMR spectroscopy (Supporting Information, Figures S26–S29). The extent of degradation was quantified using Equation S5 and plotted in Figure S30.

Compound **HB** began degrading immediately after its dissolution in the basic solution at room temperature and was

[*] A. G. Wright, T. Weissbach, Prof. S. Holdcroft
Department of Chemistry, Simon Fraser University
8888 University Dr., Burnaby BC, V5A 1S6 (Canada)
E-mail: holdcrof@sfu.ca

Supporting information for this article can be found under http://dx.doi.org/10.1002/anie.201511184.

  

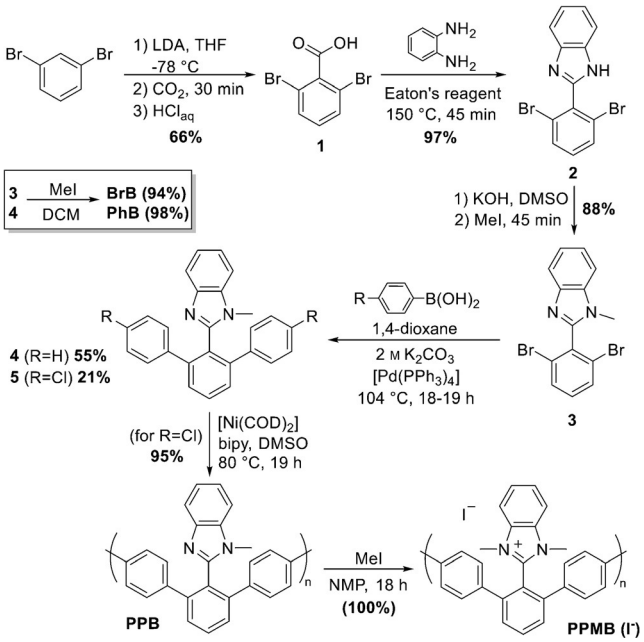


***Scheme 1.*** Synthetic route to the model compounds (**BrB** and **PhB**) and polymers **PPB** and **PPMB**.

fully degraded to its amide product by time of the first measurement (Figure S29), demonstrating extreme lability of unprotected benzimidazoliums in strongly alkaline media.

**BrB** appeared to be stable at room temperature, but fully degraded after 17 h when the temperature was raised to 80 °C (Figure S28). The transition of the resonance from 4.00 ppm to 3.90 ppm in the $^1$H NMR spectrum suggests that new dimethylated benzimidazoliums are produced, which form from the nucleophilic displacement of bromide for hydroxy groups, as well as amide products, which appear at 3.0–2.7 ppm.

Degradation of **MeB** and **PhB** followed exponential decay, indicative of a pseudo-first order reaction. By fitting the data to exponential functions, the rate constants and half-life ($t_{1/2}$) at 80 °C in those solutions were calculated, as shown in Table 1. The rate of degradation of **PhB** ($t_{1/2}$ 3240 h) was ≈ 7 times slower than that of **MeB** ($t_{1/2}$ 436 h), which represents the highest alkaline stability for a benzimidazolium hydroxide reported to date.

Motivated by the stability of **PhB**, we designed a synthetic route to prepare the polymeric analogue, **PPMB** (Scheme 1). The neutral polymer, **PPB**, was prepared by Yamamoto coupling of **5** to produce a high-molecular-weight (intrinsic viscosity of 2.10 dL g$^{-1}$; Figure S25) poly(phenylene) backbone bearing 1-methylbenzimidazole pendant groups. If the intrinsic viscosity of **PPB** dissolved in *N*-methyl-2-pyrrolidone behaved similarly to that of poly(benzimidazole) in *N*,*N*-dimethylformamide, which has Mark–Houwink constants $a = 0.75$ and $K_w = 3.2 \times 10^{-4}$ dL g$^{-1}$,[23] **PPB** would have a molecular weight of 129000 g mol$^{-1}$. Complete methylation of **PPB** with iodomethane produced **PPMB** in its iodide form. As a membrane, **PPMB** was strong and flexible, possessing a high tensile strength of 72 MPa, elongation at break of 49 %, and Young's modulus of 1.29 GPa (Figure S37). In its hydroxide form, the colorless and transparent film possessed an ion-exchange capacity ($IEC_{OH^-}$) of 2.56 meq g$^{-1}$. In its fully hydrated state and in air, it exhibited a mixed hydroxide/carbonate conductivity of 13.2 ± 1.4 mS cm$^{-1}$ (22 °C), which is twice the conductivity of methyl-protected poly(benzimidazolium) of similar IEC and similar water uptake of 81 ± 10 %.[19] Additionally, the conductivity is in the same order of magnitude as that of pendant alkyl ammoniums and imidazoliums.[24–28] After immersion of the membrane in 1 M or 2 M KOH at 80 °C for 168 h, only 1.7 % and 5.3 % degradation was observed, respectively (Figure S35), which is unprecedented for a benzimidazolium-containing polymer. A plot of the stability of **PPMB** in 2 M KOH at 80 °C over time is shown in the Supporting Information, Figure S36, which did not appear to follow first-order kinetics. As this is unlike the small molecule stability tests, we presume that this is due to the distinct differences between homogeneous and heterogeneous degradation experiments.

***Table 1:*** Properties of the model compounds based on experimental data and DFT calculations.

| Compound | Solid-state dihedral angle[a] | Solution-state dihedral angle[b] | C2–I$^-$ [Å][c] | $t_{1/2}$ [h][d] |
|---|---|---|---|---|
| **HB** | 54.40/55.02 | 62 | 3.704 | < 0.1 |
| **BrB**[e] | 70.45/73.26 | 88 | 5.497 | < 10 |
| | 73.08/81.92 | | 5.587 | |
| **MeB** | 79.21/83.77 | 86 | 4.743 | 436 |
| **PhB** | 65.03/68.58 | 71 | 6.218 | 3240 |

[a] Measured between the benzimidazolium and C2 phenyl planes in the iodide form from XRD below 90°. [b] DFT calculated solution structures. [c] The shortest C2 carbon–iodide distance(s) for the iodide-form X-ray structures. [d] The half-life of the compound dissolved in 3 M NaOD/$CD_3OD/D_2O$ at 80 °C. [e] **BrB** (XRD) possessed two unique structures within one unit cell.

To investigate the origin of the stability differences between the C2-protected benzimidazolium small molecules, single crystals were grown and characterized by XRD. Furthermore, the structures were compared to those found using DFT calculations. Each compound was crystallized in its iodide form. The methods for their crystallization as well as their relevant crystal data can be found in the Supporting Information, Table S1. Refined crystal structures are shown in Figure 2. Using the crystal structures, the dihedral angles between the benzimidazolium plane and that of the C2-substituted phenyl plane (Figure S38), as well as the shortest distance between the C2 carbon and iodide, were measured (Table 1).

The solid-state dihedral angles within each molecule were unique for each quadrant owing to the non-planarity of the benzimidazolium ring. **BrB** possessed the largest variation of dihedral angles, and also possessed two molecular structures in its unit cell, leading to eight different dihedral angles. The average dihedral angles increased in the order **HB** < **PhB** < **BrB** < **MeB**. As this trend does not follow the trend in half-life in strong base, the dihedral angle alone cannot be used as a measure of hydroxide stability. However, the C2 carbon–iodide distance does match the trend in half-life, with the longer distance translating to a longer half-life. The exception to this trend is **BrB**, as its protecting bromine groups are strongly susceptible to nucleophilic displacement.

  

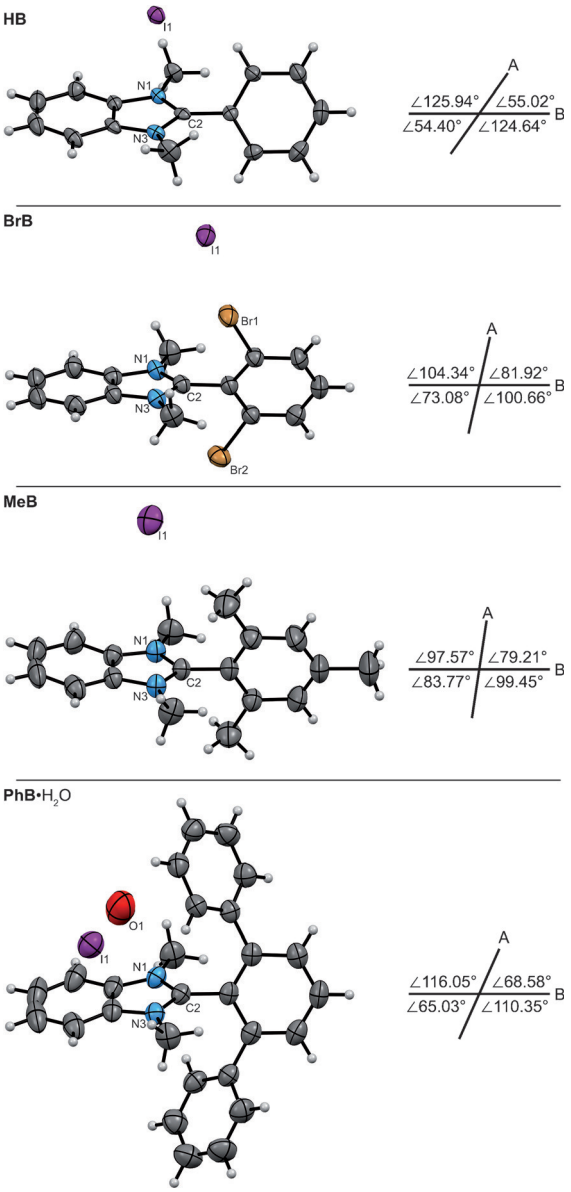


***Figure 2.*** X-ray crystal structures[29] of model compounds in their iodide form (ellipsoids set at 50% probability) alongside the dihedral angles measured (**A** represents the 2-phenyl plane and **B** represents the benzimidazolium plane). Only one of the two unique **BrB** structures is shown for clarity and **PhB** co-crystallized with $H_2O$ (where the hydrogen atoms of $H_2O$ are not shown).

To compare the hydroxide stability differences between **HB**, **MeB**, and **PhB**, DFT was used to calculate the energy barriers and states along two possible degradation pathways, which are graphically displayed in Figure 3 (see Table S2 for values). The overall reaction for each pathway is shown in Scheme 2. The first pathway represents the nucleophilic addition–elimination reaction of hydroxide on the C2 carbon of the benzimidazolium, resulting in the amide "ring-opened" product. The second pathway represents the nucleophilic substitution of hydroxide with the *N*-methyl carbon, resulting in a 2-substituted-1-methylbenzimidazole, which we term "de-methylation" degradation.

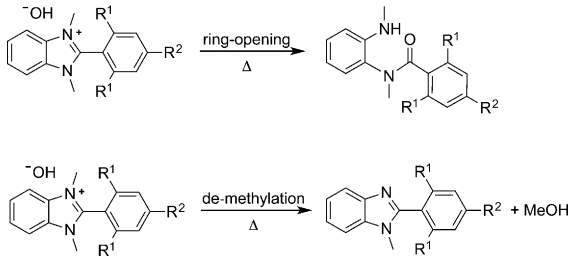


***Scheme 2.*** The two degradation pathways for benzimidazolium hydroxides (ring-opening and de-methylation).

As observed in Figure 3, the nucleophilic addition–elimination reaction on the C2 carbon of the benzimidazolium leads to the formation of an intermediate state ($IS_1$) after overcoming the first transition state ($TS_1$). **HB** has a reaction free energy barrier ($\Delta G^{\ddagger}$) of 10.6 kcal mol$^{-1}$ for $TS_1$, which is considerably lower in energy compared to **MeB** (22.9 kcal mol$^{-1}$), and is similar to findings of Long and Pivovar. As $\Delta G^{\ddagger}$ is greatest for $TS_1$, the higher the energy for this rate-limiting step, the slower the ring-opening degradation. As such, **MeB** should have improved stability over that of **HB**, which is in good agreement with experimental observation. **PhB** is even more resistant to ring-opening degradation, consistent with the larger $\Delta G^{\ddagger}$ (24.2 kcal mol$^{-1}$).

The second transition state ($TS_2$) may proceed by one of two ways depending on the orientation of the two *N*-methyl groups ($TS_{2,trans}$ or $TS_{2,cis}$) and results in two different configurational isomers of the amide product (Figures S40, S41). The $^1$H NMR spectra of degraded **MeB** reveal numerous amide products being formed, as only two alkyl peaks are expected for a single isomer configuration in the 3.0–2.0 ppm resonance region. Degraded products were also isolated (see the Supporting Information for methods) and analyzed by mass spectrometry (Figure S31). Only the amide product was observed, with various amounts of deuterium exchange on the methyl groups. However, when the same process was performed on the isolated **PhB** degradation products, two products were observed (Figure S32) that were not present in the mass spectrum prior to the degradation test (Figure S34). The ring-opened amide was present alongside the de-methylated product, which is the first observation of its kind for an alkali-degraded benzimidazolium hydroxide.

DFT calculations indicated that the activation energies of de-methylation differ only slightly between **HB**, **MeB**, and **PhB** ($\Delta G^{\ddagger}$ of $TS_{SN2}$ of 27.4, 26.9, and 27.3 kcal mol$^{-1}$, respectively). As $TS_1$ is generally significantly lower than $TS_{SN2}$, the de-methylation product is usually not observed. However, the substantial increase in the $\Delta G^{\ddagger}$ of $TS_1$ for **PhB** has decreased the energetic advantage of ring-opening degradation over that of de-methylation, with a difference of only 3.1 kcal mol$^{-1}$. While the effects of methanol were not considered in the DFT calculations, the estimated differences between the degradation rate and mechanism of individual model compounds are in good agreement between DFT and experiment.

In summary, through examination of benzimidazolium hydroxide model compounds, XRD, and DFT calculations,

  

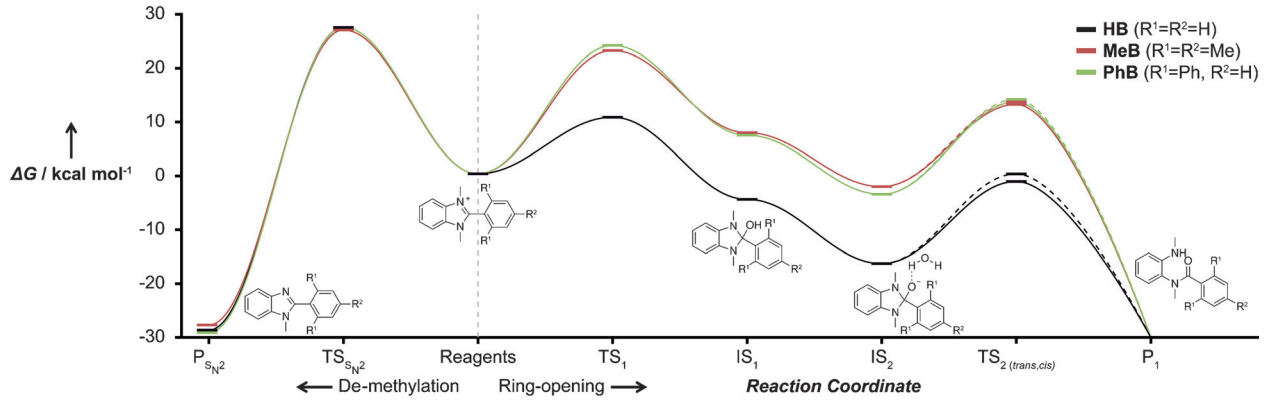


***Figure 3.*** Reaction profiles for the two hydroxide-mediated degradation pathways (de-methylation and ring-opening) for **HB**, **MeB**, and **PhB**. The dotted lines represent the higher energy, $TS_{2,cis}$, ring-opening degradation pathway. No barrier was found between $IS_1$ and $IS_2$.

the effect on stability of four C2-protecting groups have been rationalized. A benzimidazolium is designed to be pendant on a poly(phenylene)-backbone in a manner that makes use of the sterically-protecting function of *ortho*-disubstituted phenylenes. Such polymers provide exceptional stability in alkaline solutions at 80 °C. Moreover, a versatile synthetic route is presented that facilitates further investigations of numerous other C2-protecting groups.

## Acknowledgements

This work was financially supported by the Natural Sciences and Engineering Research Council of Canada (NSERC). We thank Dr. Jeffrey S. Ovens and Prof. Daniel B. Leznoff for XRD training. Computing resources were provided by WestGrid (www.westgrid.ca) and Compute Canada Calcul Canada (www.computecanada.ca).

**Keywords:** alkaline stability · anion exchange membranes · benzimidazolium · fuel cells · nitrogen heterocycles

**How to cite:** *Angew. Chem. Int. Ed.* **2016**, *55*, 4818–4821
*Angew. Chem.* **2016**, *128*, 4898–4902

[1] J. R. Varcoe, R. C. T. Slade, E. Lam How Yee, S. D. Poynton, D. J. Driscoll, D. C. Apperley, *Chem. Mater.* **2007**, *19*, 2686–2693.
[2] N. Li, Y. Leng, M. A. Hickner, C.-Y. Wang, *J. Am. Chem. Soc.* **2013**, *135*, 10124–10133.
[3] J. Wang, S. Gu, R. B. Kaspar, B. Zhang, Y. Yan, *ChemSusChem* **2013**, *6*, 2079–2082.
[4] F. Gu, H. Dong, Y. Li, Z. Si, F. Yan, *Macromolecules* **2014**, *47*, 208–216.
[5] M. Zhang, J. Liu, Y. Wang, L. An, M. D. Guiver, N. Li, *J. Mater. Chem. A* **2015**, *3*, 12284–12296.
[6] A. D. Mohanty, C. Y. Ryu, Y. S. Kim, C. Bae, *Macromolecules* **2015**, *48*, 7085–7095.
[7] P. Jannasch, *ECS Trans.* **2015**, *69*, 369–375.
[8] H. P. Gregor, J. Belle, R. A. Marcus, *J. Am. Chem. Soc.* **1955**, *77*, 2713–2719.
[9] O. I. Deavin, S. Murphy, A. L. Ong, S. D. Poynton, R. Zeng, H. Herman, J. R. Varcoe, *Energy Environ. Sci.* **2012**, *5*, 8584–8597.
[10] X. Lin, X. Liang, S. D. Poynton, J. R. Varcoe, A. L. Ong, J. Ran, Y. Li, Q. Li, T. Xu, *J. Membr. Sci.* **2013**, *443*, 193–200.
[11] D. Pletcher, X. Li, *Int. J. Hydrogen Energy* **2011**, *36*, 15089–15104.
[12] M. Skyllas-Kazacos, M. H. Chakrabarti, S. A. Hajimolana, F. S. Mjalli, M. Saleem, *J. Electrochem. Soc.* **2011**, *158*, R55–R79.
[13] G. Z. Ramon, B. J. Feinberg, E. M. V. Hoek, *Energy Environ. Sci.* **2011**, *4*, 4423–4434.
[14] J. R. Varcoe, P. Atanassov, D. R. Dekel, A. M. Herring, M. A. Hickner, P. A. Kohl, A. R. Kucernak, W. E. Mustain, K. Nijmeijer, K. Scott, et al., *Energy Environ. Sci.* **2014**, *7*, 3135–3191.
[15] M. G. Marino, K. D. Kreuer, *ChemSusChem* **2015**, *8*, 513–523.
[16] O. D. Thomas, K. J. W. Y. Soo, T. J. Peckham, M. P. Kulkarni, S. Holdcroft, *J. Am. Chem. Soc.* **2012**, *134*, 10753–10756.
[17] H. Long, B. Pivovar, *J. Phys. Chem. C* **2014**, 118, 9880–9888.
[18] K. M. Hugar, H. A. Kostalik, G. W. Coates, *J. Am. Chem. Soc.* **2015**, *137*, 8730–8737.
[19] A. G. Wright, S. Holdcroft, *ACS Macro Lett.* **2014**, *3*, 444–447.
[20] T. Zimmermann, K. Schmidt, *J. Heterocycl. Chem.* **1996**, *33*, 1717–1721.
[21] Zimmermann and Schmidt synthesized 2,4,6-substituted-aryl-protected benzimidazoliums but these were never investigated for ion-exchange properties nor were hydroxide versions formed.
[22] C. Heiss, E. Marzi, M. Schlosser, *Eur. J. Org. Chem.* **2003**, *2003*, 4625–4629.
[23] Y. Yuan, F. Johnson, I. Cabasso, *J. Appl. Polym. Sci.* **2009**, *112*, 3436–3441.
[24] C. G. Arges, L. Wang, M. Jung, V. Ramani, *J. Electrochem. Soc.* **2015**, *162*, F686–F693.
[25] Y. Yang, J. Wang, J. Zheng, S. Li, S. Zhang, *J. Membr. Sci.* **2014**, *467*, 48–55.
[26] B. Lin, H. Dong, Y. Li, Z. Si, F. Gu, F. Yan, *Chem. Mater.* **2013**, *25*, 1858–1867.
[27] A. L. Ong, S. Saad, R. Lan, R. J. Goodfellow, S. Tao, *J. Power Sources* **2011**, *196*, 8272–8279.
[28] J. Zhou, M. Ünlü, I. Anestis-Richard, P. A. Kohl, *J. Membr. Sci.* **2010**, *350*, 286–292.
[29] CCDC 1439721 (**HB**), 1439723 (**BrB**), 1439722 (**MeB**), and 1439724 (**PhB**·$H_2O$) contain the supplementary crystallographic data for this paper. These data are provided free of charge by The Cambridge Crystallographic Data Centre.

Received: December 2, 2015
Revised: January 18, 2016
Published online: March 7, 2016

  